International Journal of Applied Electromagnetics and Mechanics 64 (2020) 119–127
DOI 10.3233/JAE-209314
IOS Press

A hybrid wind energy harvester using a slotted cylinder bluff body

Junlei Wang[a,b,†], Guoping Li[a], Zunlong Jin[a,†], Guobiao Hu[b], Kun Zhang[c] and Peng Zhang[d,*]
[a]*School of Mechanical and Power Engineering, Zhengzhou University, Zhengzhou, China*
[b]*Department of Mechanical Engineering, The University of Auckland, Auckland, New Zealand*
[c]*State Key Laboratory of NBC Protection for Civilian, Beijing, China*
[d]*School of Water Conservancy and Engineering, Zhengzhou University, Zhengzhou, China*

Abstract. Harvesting energy from wind to supply low-power consumption devices has attracted numerous research interests in recent years. However, a traditional vortex-induced vibration energy harvester can only operate within a limited range of wind speed. Thus, how to broaden the effective wind speed range for energy harvesting is a challenging issue. In this paper, a slotted cylinder bluff body is proposed for being used in the design of a wind energy harvester. The physical prototype is manufactured and the wind tunnel test is performed for evaluating the actual performance of the prototyped energy harvester. The effect of the orientation of the slot on the performance of the proposed energy harvester is experimentally investigated. As compared to the traditional counterpart without the slot at the lateral side of the bluff body, the proposed energy harvester demonstrates the superiority for realizing broadband energy harvesting. Due to the introduction of the slot, and by carefully tuning the orientation of the slot, both the vortex-induced vibration and the galloping phenomena can be stimulated within two neighboring wind speed ranges, leading to the formation of an extremely broad bandwidth for energy harvesting.

Keywords: Wind energy harvesting, slotted bluff body, vortex-induced vibration, galloping

1. Introduction

Fluid-induced vibration phenomenon has been widely investigated for the application in energy harvesting in recent years [1–10], since it has a promising potential to replace traditional chemical batteries for supplying low-power consumption devices e. g., wireless sensors and micro-electromechanical systems (MEMS) [11–27]. Though there are several different means to make the mechanical-to-electrical conversion, due to the ease of implementation and the high energy density, using piezoelectric materials to convert fluid-induced vibration into electrical energy has attracted the most research interest. According to the underlying mechanism, fluid-induced vibration can be further classified into galloping and vortex-induced vibration. Wang et al. [28] studied a vortex-induced vibration piezoelectric energy harvester (VIVPEH) and developed a lumped parameter model to describe the system. The matrix coefficient method was used to obtain the vibration response and quasi-steady state form of the output voltage.

*Corresponding author: Peng Zhang, School of Water Conservancy and Engineering, Zhengzhou University, Zhengzhou, China. Tel.: +86 13783440796; E-mail: zhangpeng@zzu.edu.cn.
†These authors contribute equally to this work.

Mehmood et al. [29] numerically investigated the vortex-induced vibration response at $96 \leq Re \leq 118$ and $0.5\ \text{M}\Omega \leq R \leq 5\ \text{M}\Omega$, the results showed that the load resistance has a significant effect on the oscillation amplitude, lift coefficient and voltage output. It was demonstrated that there is an optimum value of the load resistance for which the maximum harvested power can be achieved. Bernitsas et al. [30,31] firstly proposed the basic concept of the vortex-induced vibration aquatic clean energy converter and fabricated a physical prototype. They established a mathematical model and calculated the design parameters for various application scales. Huynh et al. [32] studied a bistable vortex-induced vibration energy harvester which was modelled as a four-dimensional autonomous continuous-time dynamical system. On the other hand, compared with vortex-induced vibration based energy harvesters, galloping piezoelectric energy harvesters (GPEH) normally can generate more energy from the surrounding environment. Yang et al. [33] tested different bluff bodies with various cross-sections for galloping energy harvesting. Their experimental results demonstrated that using square-sectioned bluff body yielded the lowest cut-in wind speed of 2.5 m/s and the highest peak power of 8.4 mW. Hu et al. [34] experimentally studied the performance of a galloping piezoelectric energy harvester with two small rod-shaped accessories installed on a main cylinder. Results showed that the energy could be harvested continuously beyond the critical wind speed and was dramatically superior over both the plain circular cylinder at circumferential locations of 45° and 60°. In addition, Hu et al. [35] measured the aerodynamic force coefficients and found that the circular cylinder with triangular rods at the location of 60° had larger transverse force coefficients than the other two rod type cases. Recently, Wang et al. [36] experimentally and numerically investigated the energy harvesting from airflows in HVAC system based on galloping of isosceles triangle sectioned bluff bodies.

Researches on wind energy harvesting using innovative structures have attracted lots of interests. Allen et al. [37] proposed an "eel" shaped flow energy harvester. Later on, Cha et al. [38] designed a bionic fish tail to harvest energy from its impact and then proposed a modeling framework for underwater vibration of bionic tail. The feasibility of the model to obtain energy was predicted theoretically and validated experimentally. Chen et al. [39] experimentally investigated the aerodynamic forces and flow structures of bionic cylinders based on harbor seal vibrissa, and it was found that a drag reduction of 15% and a maximum fluctuating lift suppression of 58% were achieved when the angle of the incoming airflow was 0°, which has a potential for the prospective application in the field of energy harvesting. Meanwhile, Pan et al. [40] studied a circular cylinder with an opening and concave surface through experiment and simulation. The results indicated an increase of the induction frequency of the modified cylinder from 2.7 to 2.9 Hz and the peak voltage from 0.35 to 0.41 V. In recent studies, Wang et al. [41,42] designed a passive turbulence control (PTC) device and attached a "Y" shaped attachment to enhance wind energy harvesting. Compared with smooth cylinder, the output power increased from 0.03 mW to 0.058 mW and 0.25 mW to 0.576 mW, respectively. Jin et al [43] added pits and hemispheric protrusions to the surface of smooth cylinder and test in the wind tunnel, experimental results show that the threshold speed decelerates from 1.8 m/s to 1 m/s, and the peak voltage reached 47 V. The abovementioned comparison revealed that the complex non-uniform surface changing the regular vortex shedding process, which may also explain the mechanism of shifting from VIV to galloping and the aerodynamic force response.

In the present work, an innovative slotted cylinder bluff body is investigated to enhance the wind energy harvesting performance. The physical prototype is manufactured and tested in wind tunnel experiments to explore the effect of the slot orientation direction on the performance of the energy harvester. The rest of the paper is organized as follows. In Section 2, the general distributed parameter modelling methods for the traditional vortex-induced vibration based energy harvester and galloping based energy harvester are briefly reviewed. However, due to the untraditional design of the bluff body, the previous

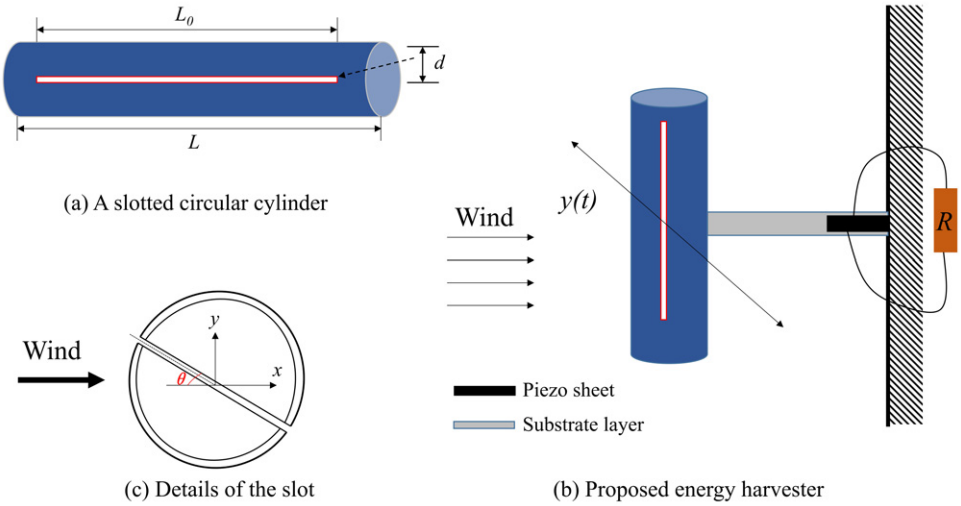

Fig. 1. Schematic of the proposed wind energy harvester.

equations for describing the aeroelastic forces caused by VIV and galloping can not be directly used. In Section 3, we presented the prototyped physical model of the proposed energy harvester and the wind tunnel experimental results. A parametric study is conducted for revealing the effect of the slot orientation direction on the performance of the proposed energy harvester. Finally, Section 4 presents the relevant conclusions and discussions.

2. System modelling

Figure 1 demonstrates the schematic of the proposed energy harvester which consists of a cantilevered beam bonded with a piezoelectric transducer at the clamped end. A cylinder of mass M_{eqm} and length L is attached at the tip of the cantilevered beam for acting as the bluff body. A through slot of width d and length L_0 is machined at the lateral side of the cylinder. Assuming that the wind speed is of U and the wind direction is along the x-axis, the orientation of the slotted cylinder is characterized by the angle θ between the slot and the wind direction. It is well known that around the fundamental natural frequency, the cantilevered beam with tip mass (i.e., the bluff body) can be approximated as a single-degree-of-freedom (SDOF) system. The effective stiffness and damping coefficient of the SDOF representation model are denoted by K_{eqs} and C_{eqd}, respectively. C_p, β represent the clamped capacitance and electro-mechanical coupling coefficient of the energy harvester. The piezoelectric transducer is shunted to a resistor R_{eqr}.

2.1. Governing equations

For a general VIV based PEH, a distributed parameter model for describing the dynamic motion of the electromechanical system can be given as [44–46]:

$$\ddot{\eta}(t) + 2\zeta\omega_n\dot{\eta}(t) + {\omega_n}^2\eta(t) + \chi V(t) = f_{\eta viv}(t) \tag{1}$$

where $\eta(t)$ is the model coordinate, and the aeroelastic force caused by VIV can be expressed as

$$f_{\eta viv}(t) = 0.25C_L\varphi(L_C)\rho DLU^2 q(t) - 0.5C_D\rho DLU\varphi^2(L_C)\dot{\eta}(t) \tag{2}$$

in which C_L, C_D are constants that can be determined by wind tunnel tests, $\phi(x)$ is the model shape function of the cantilevered beam, L_C is the length of the cantilevered beam, ρ is the air density, and q (t) is the variable in the Van Del Pol wake oscillator model for describing the VIV effect [43].

$$\ddot{q}(t) + \varepsilon\omega_f[q^2(t) - 1]\dot{q}(t) + {\omega_f}^2 q(t) = \frac{A}{D}\varphi(L_C)\ddot{\eta}(t) \tag{3}$$

where ϵ and A are also constants and can be obtained experimentally. By introducing $\eta(t)\phi(L_C) = y$ (t), $M_{eqm1} = 1/\phi^2(L_C)$, $C_{eqd1} = 2\zeta_1\omega_{n1}/\phi^2(L_C)$, $K_{eqs1} = \omega_{n1}^2/\phi^2(L_C)$, $\beta_1 = \chi/\phi(L_C)$ and rearranging Eq. (3), the reduced lumped parameter model can be obtained as follows [43].

$$M_{eqs1}\ddot{y}(t) + (C_{eqd1} + 0.5C_D\rho DLU)\dot{y}(t) + K_{eqs1}y(t) + \beta_1 V(t) - 0.25C_L\rho DLU^2 q(t) = 0 \tag{4}$$

$$\ddot{q}(t) + \varepsilon\omega_f[q^2(t) - 1]\dot{q}(t) + {\omega_f}^2 q(t) = \frac{A}{D}\ddot{y}(t) \tag{5}$$

where $M_{eam1} = (33/140)M_1 + M_2$, M_1, M_2 are the masses of the cantilevered beam and bluff body, respectively. A good approximation for the aerodynamic force model is to assume it is solely dependent on the instantaneous relative velocity and angle of attack. Note that the quasi-static hypothesis is only applicable when the characteristic timescale of the flow is small as compared to the characteristic timescale of the oscillation [47,48]. The resultant vertical aerodynamic force of GPEH system, $f_{\eta galloping}$ is thus defined as [42]:

$$f_{\eta galloping}(t) = \frac{1}{2}\varphi(L_C)\rho DLU^2 \sum_{i=1,2,\ldots} a_i \left[\frac{\dot{\eta}(t)\varphi(L_C)}{U} + \varphi'(L_C)\eta(t)\right]^i \tag{6}$$

where a_i is a semi-empirical constant depending on the cross-sectional shape. Assuming that $D \ll L_C$, the influence of the cantilever beam rotation angle is negligible, then $\phi'(L_C)\eta(t) \approx 0$. Thus, the distributed parameters model of galloping can be similarly simplified as

$$M_{eqm2}\ddot{y}(t) + \left[C_{eqd2} - \frac{1}{2}a_1\rho LDU - \frac{1}{2}a_3\rho LD\frac{\dot{y}^2(t)}{U}\right]\dot{y}(t) + K_{eqs2}y(t) + \beta_2 V(t) = 0. \tag{7}$$

2.2. Determination of equivalent lumped parameters

A prototype of the proposed energy harvester is manufactured and a wind tunnel test is performed to determine the equivalent lumped parameters of the proposed energy harvester. The prototyped energy harvester is as shown in Fig. 2(a). Figure 2(b) shows the enlarged view of the slotted cylinder bluff body that is made of foam. The cross-sectional radius and length of the cylinder bluff body are 120 mm and 16 mm, respectively. The length and the width of the lateral slot are 50 mm and 8 mm, respectively. According to the principle of piezoelectric effect, it is known that a larger stress generates a higher voltage. The clamped root of the cantilevered beam obviously bears the maximum stress when it is deflected. Thus, a piezoelectric sheet (MFC) is bonded onto the cantilevered beam at the clamped root to achieve the best energy conversion performance.

Through the free-decay test, we can determine the fundamental natural frequency and the damping ratio of the prototyped energy harvester. Fig. 2(c) shows the setup for the free-decay test. A laser sensor

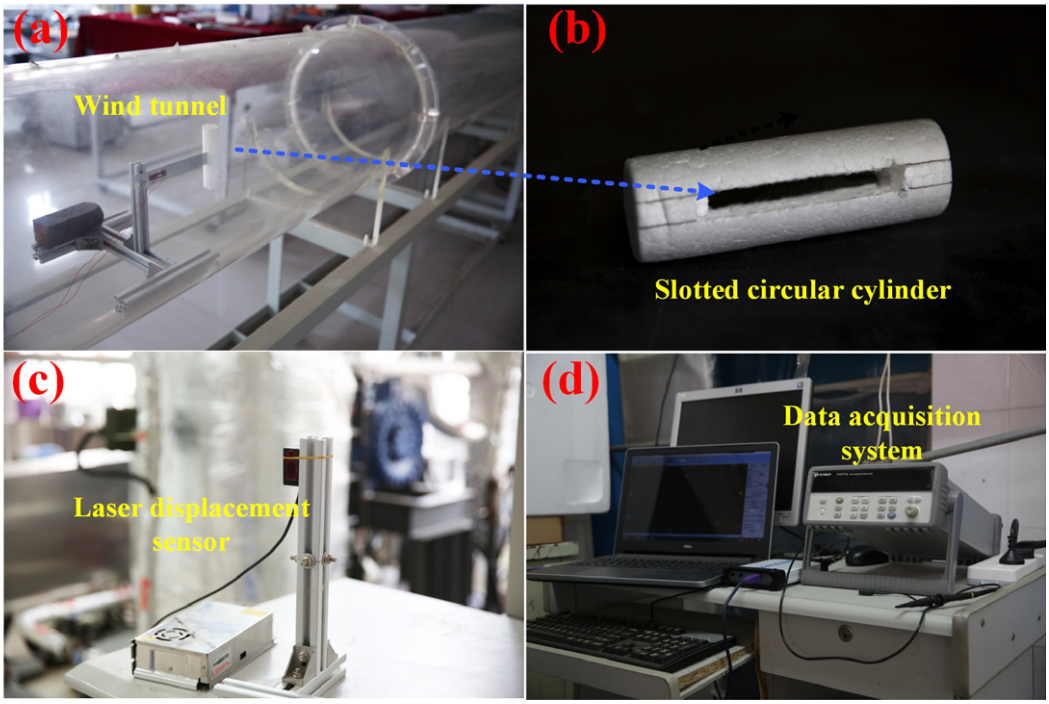

Fig. 2. (a) Installation of the prototyped energy harvester in the wind tunnel, (b) enlarged view of the slotted cylinder bluff body, (c) free-decay test setup, (d) data acquisition system.

is used to measure the displacement. Figure 2(d) shows the setup of the data acquisition system. In the experiment, the two electrodes of the piezoelectric transducer are connected to an oscilloscope which is linked to a laptop for recoding the voltage output response from the piezoelectric transducer. The other parameters related to the aeroelastic forces could not be determined, since Eqs (2) and (7) are empirical equations on the assumption that the bluff body is a traditional cylinder without the slot at the lateral side.

3. Results and analysis

As aforementioned that the theoretical modelling method only validates under the assumption of using the cylinder bluff body without the slot at the lateral side. Therefore, for the proposed energy harvester using the slotted cylinder bluff body, the following analysis and result are all based on the experimental results.

Figure 3(a) shows the time history response of the free-decay test when $\theta = 0°$. Figure 3(b) shows the frequency domain responses of the proposed energy harvester for various orientation directions of the bluff body. The result of the case without slot is also provided. It is noted that the change in the orientation direction of the bluff body i.e., θ results in the variation in the natural frequency of the proposed energy harvester. This can be explained by that for different orientation, the bluff body (i.e., the through slot) has different moment of inertia.

For different wind speed, Fig. 4 shows the voltage output responses of the proposed energy harvester with different orientation of bluff body. It can be observed that after the introduction of the slot, the

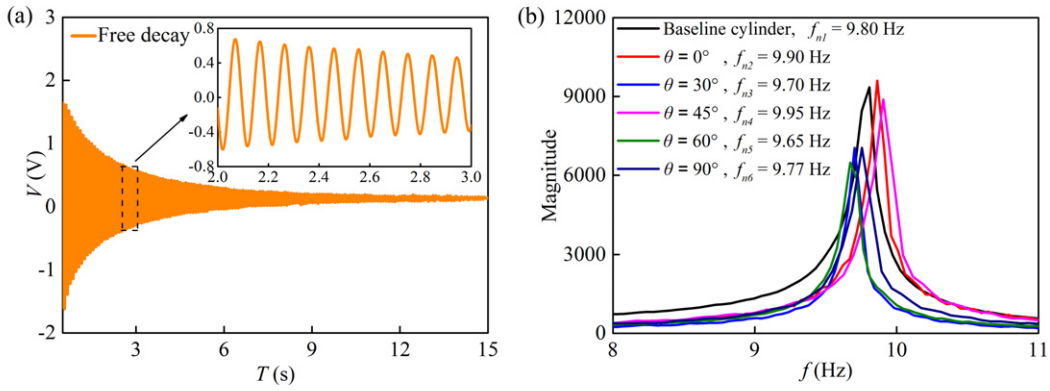

Fig. 3. Free decay test: (a) Voltage history; (b) Natural frequencies of different models.

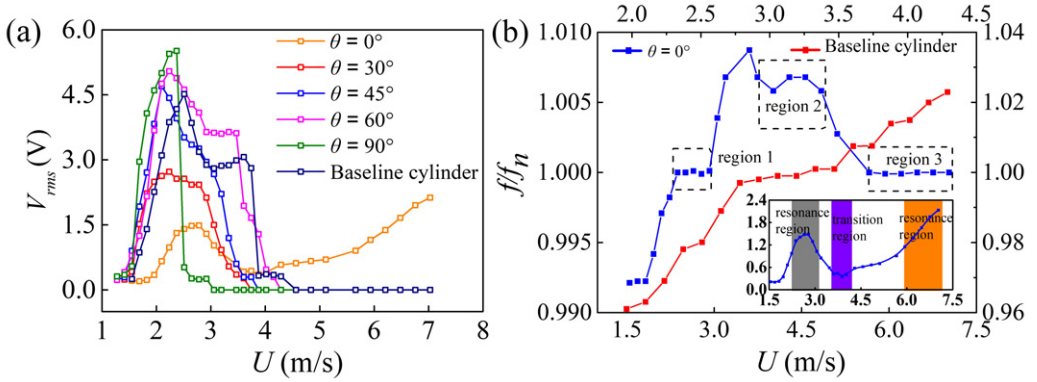

Fig. 4. Experimental results (a) voltage versus wind speed, (b) dominant oscillation frequency versus wind speed.

performance of the harvester is dramatically changed. Furthermore, the orientation of the bluff body i.e., θ, has a crucial effect on the performance of the proposed energy harvester. Overall speaking, the maximum output voltage increases with the increase of θ. When the vortex shedding frequency gets close to the resonant frequency of the proposed energy harvester, it becomes synchronized with the frequency of oscillation, leading to the occurrence of self-sustained large-amplitude oscillation. The wind speed range within which such synchronization phenomenon occurs is the termed as the lock-in region. For the traditional energy harvester, the lock-in region is 1.5 m/s–4.5 m/s and the maximum open-circuit voltage amplitude is approximately 4.5 V. For the proposed energy harvester with θ = 30°, the lock-in region is 1.4 m/s–3.7 m/s. As compared to the traditional design without the slot, the lock-in region becomes narrower and the maximum open-circuit voltage is reduced from 4.5 V to 2.7 V. For the cases of θ = 45° and θ = 60°, the maximum open-circuit voltage amplitudes are 4.7 V and 5.1 V, respectively. The lock-in regions for the two cases are almost the same as that of the traditional design. For θ = 90°, the maximum voltage amplitude is increased from 4.5 V to 5.5 V as compared to the traditional design. Unfortunately, the effective wind speed bandwidth is significantly reduced to 1.4 m/s–2.9 m/s.

It is worth particularly mentioning the case of θ = 0°. Though the maximum voltage amplitude is significantly reduced to 1.5 V, an interesting phenomenon is observed. Different from the traditional VIV-based piezoelectric energy harvester which only provides a single lock-in region for energy harvesting,

with the increase of the wind speed, in the first phase the open-circuit voltage amplitude first increases, then decreases within the range of 1.6 m/s–3.6 m/s. In the second phase, after the wind speed exceeds 4 m/s the open-circuit voltage amplitude increases monotonously with the increase of the wind speed. Thus, the measured effective wind speed range covers from 1.8 m/s to 7 m/s.

It can be found that due to the presence of the slot, the proposed energy harvester breaks through the traditional VIV based energy harvester that has a narrow lock-in region for realizing energy harvesting. The potential explanation of the success of the proposed energy harvester for $\theta = 0°$ is that the aforementioned first phase corresponds to the vortex-induced vibration phenomenon and the second phase corresponds to the galloping phenomenon. Beyond a critical value larger than 4 m/s, the vortex-induced vibration mode is transformed into galloping vibration mode. To prove this speculation, a fast Fourier transform (FFT) is performed to analyze the dominant oscillation frequency of the proposed energy harvester under different wind speed. Figure 4(b) shows the result for the case of $\theta = 0°$. It can be found that when the wind speed exceeds 5.6 m/s, the dominant oscillation frequency is exactly the same of the fundamental natural frequency of the proposed energy harvester, which is a typical characteristic of the galloping vibration. The intermediate phase between the VIV and the galloping phenomena is regarded as the transition phase. To the authors best knowledge, it is the first time to report the realization of a hybrid VIV-based and galloping based piezoelectric energy harvester.

4. Conclusions

This paper has proposed a slotted cylinder bluff body for being used in the design of a novel wind energy harvester. A physical prototype has been manufactured and an experimental test has been performed to evaluate the actual performance of the proposed energy harvester. A parametric study has been conducted to investigate the effect of θ whose physical meaning is the orientation of the slot on the performance of the proposed energy harvester. Relevant comments have been provided for guiding the selection of θ. The most important finding is that when $\theta = 0°$, the vortex-induced vibration phenomenon first appears in the first phase then the galloping phenomenon occurs afterwards in the second phase with the further increase of the wind speed. The critical wind speed for the occurrence of the galloping phenomenon is just around the upper bound of the lock-in region of the vortex-induced vibration phenomenon, therefore the overall effective wind speed bandwidth for energy harvesting has been significantly increased.

Acknowledgements

This work was supported by National Natural Science Foundation of China (Grant No.: 21676257, 51977196).

References

[1] Y. Du, S. X. Zhou, X. J. Jing et al., Damage detection techniques for wind turbine blades: A review, *Mechanical Systems and Signal Processing* (2019), 106445.

[2] J.L. Wang, L.H. Tang, L.Y. Zhao et al., Equivalent circuit representation of a vortex-induced vibration-based energy harvester using a semi-empirical lumped parameter approach, *International Journal of Energy Research* (2019), 1–13, doi:10.1002/er.5228.

[3] Z.M. Yan, L.Z. Wang, M.R. Hajj et al., Energy harvesting from iced-conductor inspired wake galloping, *Extreme Mechanics Letters* **35** (2020), 100633, doi:10.1016/j.eml.2020.100633.
[4] K. Yang, J.L. Wang and D. Yurchenko, A double-beam piezo-magneto-elastic wind energy harvester for improving the galloping-based energy harvesting, *Applied Physics Letters* **115**(19) (2019), 193901, doi:10.1063/1.5126476.
[5] X.B. Shan, H.G. Tian, D.P. Chen et al., A curved panel energy harvester for aeroelastic vibration, *Applied Energy* **249** (2019), 58–66, doi:10.1016/j.apenergy.2019.04.153.
[6] L. Ding, L. Yang, Z.M. Yang et al., Performance improvement of aeroelastic energy harvesters with two symmetrical fin-shaped rods, *Journal of Wind Engineering and Industrial Aerodynamics* **196** (2020), 104051, doi:10.1016/j.jweia.2019.104051.
[7] J.L. Wang, L.F. Geng and L. Ding, The state-of-the-art review on energy harvesting from flow-induced vibrations, *Applied Energy* **267** (2020), 114902, doi:10.1016/j.apenergy.2020.114902.
[8] L.C. Zhao, H.X. Zou, G. Yan et al., A water-proof magnetically coupled piezoelectric-electromagnetic hybrid wind energy harvester, *Applied Energy* **239** (2019), 735–746, doi:10.1016/j.apenergy.2019.02.006.
[9] J.L. Wang, S.H. Gu, C.Y. Zhang et al., Hybrid wind energy scavenging by coupling vortex-induced vibrations and galloping, *Energy Conversion and Management* **213** (2020), 112835, doi:10.1016/j.enconman.2020.112835.
[10] J.T. Zhang, Z. Fang, C. Shu et al., A rotational piezoelectric energy harvester for efficient wind energy harvesting, *Sensors and Actuators A: Physical* **262** (2017), 123–129, doi:10.1016/j.sna.2017.05.027.
[11] H.X. Zou, L.C. Zhao, Q.H. Gao et al., Mechanical modulations for enhancing energy harvesting: Principles, methods and applications, *Applied Energy* **255** (2019), 113871, doi:10.1016/j.apenergy.2019.113871.
[12] C. Hou, T. Chen, Y.F. Li et al., A rotational pendulum based electromagnetic/triboelectric hybrid-generator for ultra-low-frequency vibrations aiming at human motion and blue energy applications, *Nano Energy* **63** (2019), 103871, doi:10.1016/j.nanoen.2019.103871.
[13] Y.H. Gu, W.Q. Liu, C.Y. Zhao et al., A goblet-like non-linear electromagnetic generator for planar multi-directional vibration energy harvesting, *Applied Energy* **266** (2020), 114846, doi:10.1016/j.apenergy.2020.114846.
[14] Z.Q. Lu, D.H. Gu, H. Ding et al., Nonlinear vibration isolation via a circular ring, *Mechanical Systems and Signal Processing* **136** (2020), 106490, doi:10.1016/j.ymssp.2019.106490.
[15] Y.H. Sun and Y.G. Yang, Stochastic Averaging for the Piezoelectric Energy Harvesting System With Fractional Derivative Element, *IEEE Access* **8** (2020), 59883–59890, doi:10.1109/ACCESS.2020.2983540.
[16] X.G. Guo, Y.L. Zhang, K.Q. Fan et al., A comprehensive study of non-linear air damping and "pull-in" effects on the electrostatic energy harvesters, *Energy Conversion and Management* **203** (2020), 112264, doi:10.1016/j.enconman.2019.112264.
[17] Y.L. Wang, Z.B. Yang, P.Y. Li et al., Energy harvesting for jet engine monitoring, *Nano Energy* **75** (2020), 104853, doi:10.1016/j.nanoen.2020.104853.
[18] K.Q. Fan, M.L. Cai, F. Wang et al., A string-suspended and driven rotor for efficient ultra-low frequency mechanical energy harvesting, *Energy Conversion and Management* **198** (2019), 111820, doi:10.1016/j.enconman.2019.111820.
[19] H.L. Fu, Z. Sharif-Khodaei and F. Aliabadi, A bio-inspired host-parasite structure for broadband vibration energy harvesting from low-frequency random sources, *Applied Physics Letters* **114**(14) (2019), 143901, doi:10.1063/1.5092593.
[20] K. Tao, H.P. Yi, Y. Yang et al., Origami-inspired electret-based triboelectric generator for biomechanical and ocean wave energy harvesting, *Nano Energy* **67** (2020), 104197, doi:10.1016/j.nanoen.2019.104197.
[21] S. Fang, S. Wang, S.X. Zhou et al., Exploiting the advantages of the centrifugal softening effect in rotational impact energy harvesting, *Applied Physics Letters* **116**(6) (2020), 063903.
[22] Y.P. Wu, J.H. Qiu, S.P. Zhou et al., A piezoelectric spring pendulum oscillator used for multi-directional and ultra-low frequency vibration energy harvesting, *Applied Energy* **231** (2018), 600–614.
[23] Z.S. Chen, Y.M. Xia and J. He, Elastic-electro-mechanical modeling and analysis of piezoelectric metamaterial plate with a self-powered synchronized charge extraction circuit for vibration energy harvesting, *Mechanical Systems and Signal Processing* **143** (2020), 106824, doi:10.1016/j.ymssp.2020.106824.
[24] D.M. Huang, S.X. Zhou and Z.C. Yang, Resonance mechanism of nonlinear vibrational multistable energy harvesters under narrow-band stochastic parametric excitations, *Complexity 2019* (2019), doi:10.1155/2019/1050143.
[25] H.J. Zhu, G.M. Li and J.L. Wang, Flow-induced vibration of a circular cylinder with splitter plates placed upstream and downstream individually and simultaneously, *Applied Ocean Research* **97** (2020), 102084.
[26] J.L. Wang, L.F. Geng, S.X. Zhou et al., Design, modeling and experiments of broadband tristable galloping piezoelectric energy harvester, *Acta Mechanica Sinica* **36**(3) (2020), 592–605, doi:10.1007/s10409-020-00928-5.
[27] X. Mei, S.X. Zhou, Z.C. Yang et al., A tri-stable energy harvester in rotational motion: Modeling, theoretical analyses and experiments, *Journal of Sound and Vibration* **469** (2020), 115142.

[28] J.L. Wang, G.P. Li, M. Zhang et al., Energy harvesting from flow-induced vibration: A lumped parameter model, *Energy Sources, Part A: Recovery, Utilization, and Environmental Effects* **40**(24) (2018), 2903–2913.
[29] A. Mehmood, A. Abdelkefi, M.R. Hajj et al., Piezoelectric energy harvesting from vortex-induced vibrations of circular cylinder, *Journal of Sound and Vibration* **332**(19) (2013), 4656–4667.
[30] M.M. Bernitsas, K. Raghavan, Y. Ben-Simon et al., VIVACE (Vortex Induced Vibration Aquatic Clean Energy): A new concept in generation of clean and renewable energy from fluid flow, *Journal of Offshore Mechanics and Arctic Engineering* **130**(4) (2008), 041101.
[31] M.M. Bernitsas, Y. Ben-Simon, K. Raghavan et al., The VIVACE converter: Model tests at high damping and Reynolds number around 105, *Journal of Offshore Mechanics and Arctic Engineering* **131**(1) (2009), 011102.
[32] B.H. Huynh, T. Tjahjowidodo, Z.W. Zhong et al., Design and experiment of controlled bistable vortex induced vibration energy harvesting systems operating in chaotic regions, *Mechanical Systems and Signal Processing* **98** (2018), 1097–1115.
[33] Y.W. Yang, L.Y. Zhao and L.H. Tang, Comparative study of tip cross-sections for efficient galloping energy harvesting, *Applied Physics Letters* **102**(6) (2013), 064105.
[34] G. Hu, K.T. Tse, M.H. Wei et al., Experimental investigation on the efficiency of circular cylinder-based wind energy harvester with different rod-shaped attachments, *Applied Energy* **226** (2018), 682–689.
[35] G. Hu, J.L. Wang, Z. Su et al., Performance evaluation of twin piezoelectric wind energy harvesters under mutual interference, *Applied Physics Letters* **115**(7) (2019), 073901.
[36] J.L. Wang, L.H. Tang, L.Y. Zhao et al., Efficiency investigation on energy harvesting from airflows in HVAC system based on galloping of isosceles triangle sectioned bluff bodies, *Energy* **172** (2019), 1066–1078.
[37] J.J. Allen and A.J. Smits, Energy harvesting eel, *Journal of Fluids and Structures* **15**(3-4) (2001), 629–640.
[38] Y. Cha, M. Verotti, H. Walcott et al., Energy harvesting from the tail beating of a carangiform swimmer using ionic polymer–metal composites, *Bioinspiration & Biomimetics* **8**(3) (2013), 036003.
[39] W.L. Chen, X. W. Min, D.L. Gao et al., Experimental investigation of aerodynamic forces and flow structures of bionic cylinders based on harbor seal vibrissa, *Experimental Thermal and Fluid Science* **99** (2018), 169–180.
[40] F.F. Pan, Z.K. Xu, P. Pan et al. Piezoelectric energy harvesting from vortex-induced vibration using a modified circular cylinder, in: *Proceedings of the International Conference on Electrical Machines and Systems (ICEMS)*, IEEE, 2017, pp. 1–5.
[41] J.L. Wang, G.F. Zhao, M. Zhang et al., Efficient study of a coarse structure number on the bluff body during the harvesting of wind energy, *Energy Sources, Part A: Recovery, Utilization, and Environmental Effects* **40**(15) (2018), 1788–1797, doi:10.1080/15567036.2018.1486916.
[42] J.L. Wang, S.X. Zhou, Z.E. Zhang et al., High-performance piezoelectric wind energy harvester with Y-shaped attachments, *Energy Conversion and Management* **181** (2019), 645–652.
[43] Z.L. Jin, G.P. Li, J.L. Wang et al., Design, modeling, and experiments of the vortex-induced vibration piezoelectric energy harvester with bionic attachments, *Complexity* **2019** 2019.
[44] H.D. Akaydın, N. Elvin and Y. Andreopoulos, Wake of a cylinder: A paradigm for energy harvesting with piezoelectric materials, *Experiments in Fluids* **49**(1) (2010), 291–304.
[45] H.D. Akaydin, N. Elvin and Y. Andreopoulos, The performance of a self-excited fluidic energy harvester, *Smart Materials and Structures* **21**(2) (2012), 025007.
[46] A. Abdelkefi, M.R. Hajj and A.H. Nayfeh, Phenomena and modeling of piezoelectric energy harvesting from freely oscillating cylinders, *Nonlinear Dynamics* **70**(2) (2012), 1377–1388.
[47] L. Carassale, A. Freda and G. Piccardo, Aeroelastic forces on yawed circular cylinders: Quasi-steady modeling and aerodynamic instability, *Wind & Structures* **8**(5) (2005), 373–388.
[48] L. Carassale, A. Freda and M. Marre-Brunenghi, Effects of free-stream turbulence and corner shape on the galloping instability of square cylinders, *Journal of Wind Engineering and Industrial Aerodynamics* **123** (2013), 274–280.